

This article was downloaded by:

On: 16 January 2011

Access details: *Access Details: Free Access*

Publisher *Taylor & Francis*

Informa Ltd Registered in England and Wales Registered Number: 1072954 Registered office: Mortimer House, 37-41 Mortimer Street, London W1T 3JH, UK



Journal of Energetic Materials

Publication details, including instructions for authors and subscription information:

<http://www.informaworld.com/smpp/title~content=t713770432>

The mechanical response of TNT and a composite, composition b, of TNT and RDX to compressive stress: I uniaxial stress and fracture

D. A. Wiegand^a; J. Pinto^a; S. Nicolaides^a

^a Energetics and Warheads Division Armament Engineering Directorate Armament Research, Development and Engineering Center Picatinny Arsenal, NJ

To cite this Article Wiegand, D. A. , Pinto, J. and Nicolaides, S.(1991) 'The mechanical response of TNT and a composite, composition b, of TNT and RDX to compressive stress: I uniaxial stress and fracture', *Journal of Energetic Materials*, 9: 1, 19 – 80

To link to this Article: DOI: 10.1080/07370659108019858

URL: <http://dx.doi.org/10.1080/07370659108019858>

PLEASE SCROLL DOWN FOR ARTICLE

Full terms and conditions of use: <http://www.informaworld.com/terms-and-conditions-of-access.pdf>

This article may be used for research, teaching and private study purposes. Any substantial or systematic reproduction, re-distribution, re-selling, loan or sub-licensing, systematic supply or distribution in any form to anyone is expressly forbidden.

The publisher does not give any warranty express or implied or make any representation that the contents will be complete or accurate or up to date. The accuracy of any instructions, formulae and drug doses should be independently verified with primary sources. The publisher shall not be liable for any loss, actions, claims, proceedings, demand or costs or damages whatsoever or howsoever caused arising directly or indirectly in connection with or arising out of the use of this material.

THE MECHANICAL RESPONSE OF TNT AND A COMPOSITE, COMPOSITION B, OF
TNT AND RDX TO COMPRESSIVE STRESS: I UNIAXIAL STRESS AND FRACTURE

D. A. Wiegand J. Pinto and S. Nicolaides

Energetics and Warheads Division
Armament Engineering Directorate
Armament Research, Development and Engineering Center
Picatinny Arsenal, NJ 07806-5000

ABSTRACT

The stress strain behavior, compressive strength and Young's modulus of trinitrotoluene (TNT) and a composite (Composition B) of TNT and cyclotrimethylene trinitramine (RDX) have been investigated in uniaxial compression as a function of temperature and strain rate. The compressive strengths and the moduli decrease with increasing temperature and decreasing strain rate. Limited tensile measurements were also made. Failure is by brittle fracture for all conditions investigated and can be explained in terms of the Griffith criteria for fracture. The temperature and strain rate dependence of the compressive strength can be attributed to the dependence of the modulus on these parameters and thermally activated slow subcritical crack growth before fracture.

INTRODUCTION

Little attention has been given to determining and

Journal of Energetic Materials vol. 9, 019-080 (1991)
Published in 1991 by Dowden, Brodman & Devine, Inc.

understanding the mechanical properties of molecular organic polycrystalline solids. In an effort to understand these types of materials and, in particular, to determine and understand failure conditions, the mechanical properties of trinitrotoluene (TNT) and a composite of trinitrotoluene and cyclotrimethylene trinitramine (RDX) have been investigated. Measurements have been made as a function of temperature and strain rate. Both TNT and the composite (Composition B) are very important military explosives. Knowledge of the mechanical properties and, in particular, the conditions for failure are very important relative to the safe use of these materials. The conditions of stress, strain rate and temperature experienced during cast cooling, handling, and in weapons use such as artillery launch are of special importance. Thus, studies were made for two strain rates, a quasi-static rate which is appropriate for cast cooling and some handling conditions, and a higher strain rate which is applicable to other conditions of handling and weapons use. Temperatures between 0° and 60°C were used in the studies reported in this paper. The majority of measurements were made in compression and the results for uniaxial compression are reported here. Very limited measurements were also made in uniaxial tension. Studies have also been made for triaxial confined compression and the results of these studies will be reported in a companion paper.¹ The triaxial confined conditions

simulate the conditions which the explosives experience during artillery launch.

TNT and the composite were prepared by casting from the melt. Composition B (Comp B) can be prepared by adding particulate RDX and wax to molten TNT. Comp B contains 39.4% TNT, 59.6% RDX and 1% wax. TNT and Comp B fail by brittle fracture under uniaxial loading and these materials are much weaker in tension than in compression. During the casting and cooling process defects such as cracks, porosity and larger voids or cavities are often introduced. These defects are very important because they are thought to play a critical role in, for example, premature ignition during artillery launch. Some of these defects are caused by stresses during cast cooling, e.g. thermal stresses, and mechanical properties for these conditions are needed for computer modeling so as to be able to predict conditions which will not result in defect generation. There are free surfaces because of these defects and so measurements were made for the simplest conditions of free surfaces, i.e. uniaxial stress and at a low quasi-static rate. Measurements were also made at a higher strain rate to provide the information and understanding necessary for computer modeling to predict failure conditions with defects during use, e.g., during artillery launch.

Complete stress vs. strain curves were recorded as a

function of the various parameters mentioned above and particular attention has been given to the compressive strength, Young's modulus, and also the strain at the compressive strength. The goal is to develop a basic understanding of these materials which will enable predictions of failure conditions and provide guidance for avoiding failure. Limited numbers of measurements were made for each condition of temperature and strain rate. The intent was to survey the mechanical properties as a function of these conditions to provide the bases for an understanding. Additional work with larger numbers of samples is desirable to place the results and understanding presented here on a firmer base.

Finally, it is important to note that at no time during the course of these experimental studies was any evidence of fast explosive reaction observed.

EXPERIMENTAL

Loading Apparatus

The mechanical properties experiments described in this paper were performed using a medium rate, high load, servo-hydraulic system. A schematic of the system is shown in Figure 1. A compressive or tensile load can be applied to a test specimen by hydraulically moving the actuator rod up or down. The system can apply a force of up to 35,000 lbs and can achieve a maximum free run velocity of up to 80 in/s. Strain rates of up

to 8 s^{-1} can be obtained for explosive samples of the size used in this work. Failure of a test specimen can be achieved in approximately 2 to 5 ms (see Figure 2).

The operation of the apparatus is controlled by a PDP 11/03 microcomputer. Any desired load-time, displacement-time, or strain-time profile within the limits of the system can be programmed into the computer and applied to a test specimen. The desired profile is generated with the aid of a feedback loop from the appropriate sensor, e.g., the load cell, to the computer (see Figure 1). For both the low and high strain rates the displacement was controlled. The computer also controls data acquisition, data analysis, data display, hard copy generation, and data transfer to a mass storage device. The electronics and control parts of the apparatus were isolated physically from the load frame so that explosives and propellants could be tested safely.

A linear variable differential transformer (LVDT) was used to measure the displacement of the actuator rod and thus the change in length of the sample and a load cell was used to measure the applied force. The LVDT and the load cell are calibrated annually by the manufacturer. Additional static calibrations of the LVDT were made with a machinist type dial indicator gage using increments of 0.001 in. The LVDT was also calibrated dynamically at several strain rates against strain

gages using a lucite sample.² Amplifiers were available for three sets of strain gage circuits. The crossheads were enclosed in a large insulated chamber for temperature conditioning, and the air in this chamber was either heated electrically or cooled by blowing solid carbon dioxide into the chamber. A control thermocouple regulated the flow of current to the heater or of coolant into the chamber to achieve and maintain the desired temperature. At low rates the apparatus is capable of applying constant load (stress) or displacement (strain) rates to the sample and at such rates the acceleration and deceleration are not significant. However, when the apparatus is driven to its maximum rate as it was in the work reported here for the high strain rate, the acceleration and deceleration can be significant. In order to decrease deceleration problems as the maximum displacement was approached, the apparatus was overdriven, i.e., the maximum displacement programmed into the computer was greater than that necessary to complete the desired effect, e.g., compressive failure. The stress and strain rates were not constant as a function of time for the high strain rate work since the hydraulics had to be overdriven to obtain the desired strain rate and typical curves of strain rate and stress vs. time are given in Figure 2. The strain rate data has been smoothed by averaging every nine points of the original strain rate vs. time curve. The noise in the strain rate curve

originates in the LVDT as well as contributions from analogue to digital and digital to analogue conversions required in the high rate data handling process. After the initial acceleration the strain rate has the average value of 1.4 s^{-1} . For all data given in this paper, high strain rate refers to the strain rate vs. time data of Figure 2. The low strain rate was constant at $6.7 \times 10^{-4} \text{ s}^{-1}$ to within approximately 1%.

In order to measure the uniaxial compressive properties of Comp B and TNT, cylindrically shaped test specimens were first coated on their end faces with a thin film of graphite powder in order to minimize binding and friction at the compression faces. The test specimens were then placed in the insulated temperature chamber for conditioning at approximately the desired temperature. After a suitable length of time the test specimens in sequence were placed on the lower crosshead for additional temperature conditioning. Thermocouples were attached to the top and bottom of each specimen, and a thermocouple was suspended in the air next to the specimen. These temperatures were monitored until equilibrium at the desired temperature was achieved. For extremely high temperatures heating tape was wrapped around the metal parts to bring them to the desired temperature more quickly. When the desired temperature was achieved the test specimen was slowly brought into contact with the heated upper crosshead and a small pre-stress of approximately 50 psi was

applied to the specimen to avoid impact between the specimen and the upper crosshead, especially at high rate. A displacement versus time profile was then programed into the computer and applied to the specimen.

Sample Preparation

Composition B and TNT casts were made by pouring the molten material either into a cylindrical metal split mold or into cardboard cylinders.³ The casts were cut as described below and machined to the desired sample dimensions and tolerances. The material was x-ray radiographed after casting and discarded if there were significant cracks, voids, or porosity. All samples were also radiographed after machining. Details of the casting procedures are given elsewhere.³ One cast each of TNT and Comp B were obtained for this work using the split mold.

The casts obtained from the split mold were cut into sections perpendicular to the axis and the sections from the very top and bottom of the casts were discarded.³ The remaining sections were then further cut and machined into cylindrical samples with axes either parallel to the cast axis or perpendicular to this axis. The samples were 1.5 in long and the diameters were nominally 0.752 in but samples with a range of diameters were actually obtained and these were used to make confined cylinder triaxial measurements at various

temperatures.^{1,3} The sample end surfaces were flat and parallel to ± 0.001 in.

Two different cardboard molds were used which differed only in length. One sample was obtained from each of the smaller casts and the larger casts were cut up and samples prepared in much the same manner as the casts from the split mold except that the axes of most samples obtained in this way were aligned parallel to the mold axis. In general, samples obtained from the cardboard molds were of better quality than samples obtained from the split mold and the best samples were obtained from the smaller casts.

RESULTS

Composition B

Composition B samples, some of which were cast in the split mold and others which were cast in the smaller cardboard tubes, were measured in uniaxial compression. The specimens from the smaller cardboard tubes were measured at the low and high strain rates and at 0', 23', 40', and 60'C. Measurements were also made at -20' and -40'C but the results were very erratic and non-reproducible, and are not presented. In all of these experiments axial stress and strain were measured and a modulus was calculated from the slope of the stress vs. strain curve. Stress vs. strain curves for Comp B are given in Figures 3 and 4 and photographs of typical sample fragments after failure are given in Figure 5. The compressive strength, σ_c , is taken at the

maximum of the stress vs. strain curve, ϵ_m is the strain at σ_m , and Young's modulus is taken as the slope of the straight line region as shown. The sample fragments indicate a brittle type of failure. There is some "crumbling" and "powdering" as a result of uniaxial compressive failure (not shown in Figure 5). Very extensive powdering has also been found as a result of mechanical failure of a simulated void due to an applied compressive stress.⁴ In addition, extensive powdering occurred in specimens as a result of impact.⁵

The average compressive strength at 23°C and at the high strain rate is 3260 ± 150 psi, the average strain, ϵ_m , is $0.65 \pm 0.10\%$, and the average elastic modulus is $(0.60 \pm 0.02) \times 10^6$ psi. The results at 23°C are summarized in Table 1. In general the strains, ϵ_m , were found to vary more from sample to sample than the moduli or the compressive strengths.³ This variation in the strains at failure is undoubtedly due at least in part to uncertainties inherent in the method by which they were determined. Because of the rounding of the stress vs. strain curves in the vicinity of σ_m and because of noise in the data there is more uncertainty in the determination of ϵ_m than in the determination of σ_m from the curves (see Figures 3 and 4). Although samples were machined into cylinders with axes parallel and perpendicular to the cast axis, insufficient data was

obtained to determine if there was a dependence of these mechanical properties on the orientation of the axis.³ Orientation dependence has been found for low rate measurements.⁶

TABLE 1

	RATE	Comp B	TNT
σ_m COMPRESSIVE STRENGTH (PSI)	LOW	1680	960
	HIGH	3260 ± 150	1850 ± 180
E YOUNG'S MODULUS (X 10 ⁶ PSI)	LOW	0.36	0.25
	HIGH	0.60 ± 0.02	0.45 ± 0.07
ϵ_m STRAIN AT σ_m (%)	LOW	0.49	0.45
	HIGH	0.65 ± 0.1	0.58 ± 0.07

Summary of Experimental Results at 23°C.

The results of uniaxial measurements of Comp B cast in the small cardboard tubes are given in Figure 7 for two strain rates and four temperatures. The low rate compressive strength data agree well with the data of Costain and Motto⁸ as a function of temperature and the high rate compressive strength at room temperature is in agreement with the value given by Clark and

Schmitt.⁹ These investigators made measurements on Comp B under similar loading conditions on specimens of comparable size to those used in this study. The results of Figure 7 indicate that the uniaxial compressive strength decreases with increasing temperature and decreasing strain rate (see also Figures 3 and 4). Clark and Schmitt also report a decreasing compressive strength with decreasing rate but they report a considerably greater decrease for a somewhat smaller decrease in rate.⁹

The results presented in Figures 3 and 4 indicate that the modulus also decreases with decreasing strain rate. In Figure 8 the modulus, E , is given as a function of temperature at the low and high strain rates as determined from the uniaxial measurements. The results indicate that E decreases with increasing temperature and decreasing strain rate. More extensive data obtained by triaxial compression measurements indicate the same dependence on temperature and strain rate.^{1,3} In contrast, Clark and Schmitt found no dependence of the modulus on rate.⁹ However, in later work of these investigators with more limited data as a function of rate, the modulus at four temperatures was found to be higher at the higher rate.¹⁰ There also is some indication that the strains at failure are lower at the low strain rate.³ However, as noted above, there is considerable scatter in the strains, ϵ_m . Thus, this trend as a

function of strain rate cannot be taken as too significant.

Both Clark and Schmitt^{9,10} and Costain and Motto⁸ report moduli which are significantly larger (a factor of two or more) than values reported here. Larger moduli have also been reported elsewhere.¹¹ While Clark and Schmitt¹⁰ report moduli which decrease with increasing temperature, the more limited data of Costain and Motto⁸ indicate an increase in modulus with increasing temperature. Smaller strains at failure are also reported by these investigators. The methods of sample preparation and the quality of the samples used by these investigators are unknown, although Clark and Schmitt do give sample densities and indicate that some samples were vacuum cast.^{9,10} Costain and Motto give only average densities. In addition, the stress vs. strain curves given by Clark and Schmitt show considerable curvature and Costain and Motto do not give stress vs. strain curves. In the work reported here the stress vs. strain curves are linear almost to failure (see Figures 3 and 4) and the moduli are determined by the slopes of the linear regions. The load cell and LVDT used in this work were calibrated annually by the manufacturer as noted above and have shown no significant changes over several years.

A few samples of Comp B were strain gaged and measurements made with the same apparatus to determine the modulus, E, and Poisson's ratio, ν .² In all cases the axial strains as determined

by the strain gages are smaller approximately by a factor of two than the strains as determined by the LVDT, and thus the E values obtained using the strain gage strains are larger than the E values obtained using the LVDT strains by the same factor. In contrast, the average value of ν obtained from the strain gages for the low strain rate is 0.34 which is approximately in agreement with the value obtained from the triaxial measurements at 23°C.^{1,3} Because of the calibration of the LVDT, the conclusion has been made that the results for the strain gages are in error, most probably because the glue (Eastman 910) did not establish the correct flexible contact between the Comp B and the strain gages. The same fractional error is to be expected for the radial and axial parts of the strain gage. Thus, the value of ν as obtained as a ratio of these strains is found to agree with the value as determined in the triaxial measurements. Clark and Schmitt^{9,10} used strain gages and report E values which are considerably larger than the values reported in this paper and obtained using the LVDT to measure strain as noted above. However, Clark and Schmitt also obtained larger values of E from triaxial data using an LVDT to determine the strains.¹⁰

A very limited number of measurements of Comp B in uniaxial tension were also made. These measurements were made using cylindrical samples of the same type used for the compression studies. The flat ends of the samples were attached to metal

cylinders using Eastman 910 adhesive and the metal cylinders were in turn attached to the fixed and movable crossheads using a threaded arrangement. Preliminary measurements were made at the low and high strain rates at 23°C.

The results indicate that Comp B is very weak in tension. Failure in all cases was by brittle fracture and the fracture surfaces were close to being perpendicular to the direction of the applied tensile stress. The tensile strength, σ_T , was found to be 164 ± 21 psi at the low strain rate at 23°C for eight samples. A few other samples gave extremely low values of σ_T and are not included in the above average. This value of σ_T is lower than but close to the value reported by Costain and Motto,⁸ i.e., 208 psi at 23°C. Only two measurements were made at the high strain rate, and the tensile strengths of these two samples were 470 and 480 psi respectively. These results indicate a significant increase in tensile strength with increasing strain rate. An increase in tensile strength with increasing strain rate has been reported for PETN.¹² Although failure was in the explosive (Comp B) and not in the adhesive, many of the samples loaded at both high and low rate failed close to the Comp B-adhesive interface. While no evidence for chemical reaction between Comp B and the adhesive could be detected, it is felt that these tensile measurements should be repeated using the more

standard "dogbone" type of samples.

TNT

Experiments similar to those performed on Comp B were performed on TNT. These experiments were carried out to determine the effects of adding RDX and wax to TNT to make Comp B. In addition, TNT is an important material by itself. Military grade TNT was cast in the split mold and in cardboard tubes. Measurements were made as a function of temperature and strain rate as for Comp B. At 23°C and the high strain rate the average value of the compressive strength, σ_m , is 1850 ± 180 psi, the average value of the modulus, E , is $(0.45 \pm 0.07) \times 10^6$ psi and the average value of ϵ_m is 0.58 ± 0.07 %. Thus, at 23°C and the high strain rate, the average compressive strength and modulus for TNT are smaller than the values for Comp B but the average strains, ϵ_m , are not significantly different for the two materials (see Table 1). In fact, at each temperature and at each strain rate for which measurements were made the compressive strength and the modulus for Comp B are greater than the values for TNT and the strains, ϵ_r , are approximately the same.³

The compressive strengths as a function of temperature and rate are summarized in Figure 9. σ_T decreases as temperature is increased at both rates. There is also an increase of σ_T for all four temperatures as the rate is increased so that both the

temperature and rate dependencies are the same as for Comp B. The low rate σ_m data are in agreement with the results of Costain and Motto.⁸ While there is considerable scatter in the modulus values, E does tend to decrease as temperature is increased and does increase as rate is increased.³ Although the E values are smaller than the values reported by Clark and Schmitt¹⁰ the temperature dependence is similar. The E value at 23°C and the low strain rate is also somewhat smaller than the value given by Costain and Motto⁸ and the temperature dependence appears to be opposite. Young's modulus as obtained by other techniques has also been found to be greater than the values reported in this work.¹³

Summary of Experimental Results

The compressive strength and Young's modulus are dependent on temperature and strain rate and a summary of the results at 23°C is given in Table 1. The compressive strengths and Young's moduli at each temperature and at each strain rate are smaller for TNT than for Comp B while the strains at failure are approximately the same for both materials at each temperature and at each strain rate.³ The compressive strengths and the moduli of TNT and Comp B decrease with increasing temperature and decreasing strain rate. It should be noted, however, that the strain rate sensitivity is very small, e.g., an increase in the

strain rate by a factor of approximately 2.1×10^3 results in an increase in the compressive strength by only approximately a factor of two. The increase in the moduli for this change in strain rate is even smaller. The values of the moduli for TNT and Comp B found in this work are smaller than the values reported by other investigators.

DISCUSSION

In the above summary it is pointed out that the compressive strength, σ_m , and Young's modulus, E , are functions of strain rate and temperature. Some preliminary measurements were also reported on the tensile strength, σ_T . In addition it is reported that failure in both tension and compression is by brittle fracture. In the following, a discussion of brittle fracture for both tensile and compressive loading is given and the temperature and strain rate dependencies of the compressive strength are considered. Much more complete data for E will be given in a later paper.¹ Hence, the discussion of the dependence of E on the above parameters will be given in that paper.¹

Brittle Fracture

Griffith^{4,15} was the first to suggest that brittle materials contain randomly orientated cracks and that under tensile or compressive loading stress concentrations develop at the crack tips which cause them to propagate and lead to failure

by brittle fracture. Griffith's treatment is based in part on work by Inglis¹⁶ who calculated for a thin plate the maximum tensile stress (stress concentration) at the tip of an elliptical shaped crack with major axis normal to the direction of the applied tensile stress. Griffith calculated the elastic energy change due to the presence of the crack. If W is the net decrease in energy due to the presence of the crack and $2c_c$ is the original length of the crack (major axis of the ellipse), he postulated that instability will result and the crack will propagate to fracture when $dW/dc \leq 0$. He thus obtained an expression for brittle tensile fracture as

$$\sigma_T \sqrt{c_c} = \left[\frac{2E\gamma}{\pi} \right]^{\frac{1}{2}} \quad (1)$$

where σ_T is the tensile strength, E is Young's modulus, and γ is surface energy per unit area. Griffith verified this relationship experimentally by studies on glass.¹⁴ In addition, Griffith showed that tensile stress concentrations develop near the tips of cracks orientated at other angles than normal to the applied tensile stress and that tensile stress concentrations also occur for applied compressive stresses.¹⁵ The relationship between the uniaxial tensile strength, σ_T , and the uniaxial compressive strength, σ_c is given by

$$\frac{\sigma_T}{\sigma_c} = 8 \quad (2)$$

While many of the assumptions made by Griffith in obtaining equation (1) are not valid for the experimental conditions used in this work, the ratio given by equation (2) is expected to be of more general validity. In fact, agreement with equation (1) has been found for many materials.¹⁷ For Comp B, using the limited tensile strength data presented we have at 23°C for the low strain rate $\sigma_m/\sigma_T = 9.8$ and for the high strain rate $\sigma_m/\sigma_T = 6.9$ in approximate agreement with the Griffith prediction of equation (2). From the data of Costain and Motto⁸ at a low strain rate the ratio σ_m/σ_T is 8.4 for Comp B and 8.0 for TNT at 23°C. For ten composite explosive formulations with cast TNT as the base treated by Costain and Motto this ratio is in the vicinity of 8.0 for most at 23°C, 52°C and 71°C. At -40°C and -62°C this ratio is higher apparently because of a decrease of the tensile strength with decreasing temperature in this low temperature range. Some difficulty was encountered in making the tensile measurements reported by Costain and Motto at low temperatures because of sample breakage during handling, etc., apparently due to extreme brittleness.¹⁸ It is thus possible that the tensile strengths reported by these investigators at the lower temperatures are low because of undetected flaws introduced during handling.

Several other approaches have been made to study the

strength of materials containing cracks. In particular McClinton and Walsh^{19,20,21} modified the Griffith theory by assuming that in uniaxial compression the cracks close and that a frictional force characterized by a coefficient of friction μ is developed across the crack surfaces to support shear stress. For $\mu = 1.0$ the ratio σ_m/σ_T for uniaxial stress is found to be about ten which is also in approximate agreement with many experimental results.

For uniaxial compressive loading the maximum tensile stress will develop at elliptical cracks whose major axis makes an angle of 30° with the direction of the applied stress and for zero thickness cracks the angle between the crack and the applied stresses is 45° .²² These tensile stresses are in such directions that new cracks will initiate and extend toward the direction of the applied compressive stress.²² As the new crack extends it may turn in toward the direction of the applied stress.²² In this case the stress concentration at the tip will decrease and the crack will stop growing. Alternately, the new crack, which has its own stress concentration, may branch, i.e. initiate another new crack which will also extend in the direction of the applied stress. By continued branching, a network of cracks will develop which will eventually be connected and result in fracture of the specimen into columns aligned in the direction of the applied stress. An inspection of Figure 6 will reveal that this type of

fracture behavior is observed for Comp B in uniaxial compression. The rounding of the stress vs. strain curves just before the rapid decrease of stress which indicates fracture may be due to this initiation, growth and arrest of cracks (see Figures 2, 3, 4, and 5). In some other cases the fracture surfaces for Comp B have been diagonal. The frequency of these occurrences have not been studied. This behavior may be due to the effect of frictional forces between the ends of the sample and the crosshead surfaces.

The Griffith theory is based on a two dimensional model, i.e., a crack in a thin plate. However, the problem has been considered in three dimensions for a penny shaped crack.²³ The results indicate that the boundary stresses at the crack and the surface energy differ from those of the two dimensional case by only a few percent.

In summary, the Griffith theory of crack growth leading to fracture adequately explains the observed ratios of compressive to tensile strengths for Comp B and TNT. In addition, this approach predicts the observed orientation of the fracture surfaces.

The cracks may be in the material before loading and could be caused, for example, by thermal stresses during cooling from the melt, or they may be generated during plastic deformation by slip processes and interactions of dislocations.²⁴ The rounding

of the uniaxial stress vs. strain curves just before the abrupt decrease of the stress (see Figures 3, 4 and 5), which indicates fracture, could possibly be attributed to plastic deformation due to dislocation motion. However, the yield strength obtained from triaxial measurements is a factor of two or more greater than the compressive strength.^{1,3} If yield as determined for the triaxial loading case is interpreted as indicating the onset of dislocation motion which results in plastic deformation, then in the uniaxial case dislocation motion giving plastic deformation should not begin until the uniaxial stress is equal to the yield strength.^{1,3} Since Y is greater than σ_m by a factor of two or more, it is then very unlikely that appreciable dislocation motion resulting in plastic deformation precedes fracture. Thus, the rounding of the stress vs. strain curves just before fracture cannot be attributed to dislocation motion. The rounding of the uniaxial stress vs. strain curves is most probably due to crack growth and arrest as discussed above.

It should be noted that the radial confinement used in the case of the triaxial loading, i.e. allowing negligible radial strain, inhibits crack growth and propagation. Thus, although crack propagation and fracture are observed in the case of the more standard triaxial loading, i.e. with the test specimen under hydrostatic radial pressure by a fluid during axial compression, extensive crack propagation and fracture are not expected for the

case of radial confinement. This point is discussed further in reference (1).

Temperature Dependence

An inspection of Figures 7 and 9 reveals that the compressive strengths of both Comp B and TNT decreases with increasing temperature at both strain rates. While the number of samples measured is small, it is believed that the results of Figures 7 and 9 give a true picture of the trend of the compressive strengths with temperature. The results at the low strain rate are in good agreement with the results of Costain and Motto.⁸ From equation (1) we note that based on the Griffith theory of fracture this temperature dependence of the fracture strength must be due to the temperature dependence of either or both, γ , the surface energy per unit area, and E , Young's modulus, since the crack length, $2c_c$, is assumed to be independent of temperature (see below). From Figure 8, we note that E decreases with increasing temperature for Comp B for both strain rates and more limited data for TNT³ shows that E also decreases with increasing temperature at both strain rates. Assuming for the moment that γ is independent of temperature we find from equations (1) and (2) that

$$\frac{\Delta\sigma_r}{\sigma_{r_1}} = \left[1 - \left(1 - \frac{\Delta E}{E_1} \right)^{\frac{1}{2}} \right] \quad (3)$$

where $\Delta\sigma_r = \sigma_{r1} - \sigma_{r2}$ is the difference in σ_r for two temperatures

T_1 and T_2 and $\Delta E = E_1 - E_2$ is the difference in E for the same two temperatures. By using data from Figures 7, 8 and 9 and reference (3) we find that for both Comp B and TNT at both strain rates $\Delta\sigma_m/\sigma_m$ as measured is significantly greater than $\Delta\sigma_m/\sigma_{m1}$ as calculated from equation (3). It thus seems necessary to conclude that the surface energy γ also decreases with increasing temperature.

A decrease in σ_T , the fracture strength in tension, has been reported by Congleton and Petch^{25,26} with increasing temperature for Al_2O_3 , MgO and glass. These authors attribute the decrease in σ_T with increasing temperature to a decrease in γ_R , the fracture surface energy associated with a running crack. The increase in the fracture surface energy over the intrinsic surface energy as temperature is lowered is attributed to plastic deformation associated with crack propagation. Orowan²⁷ and Irwin independently included a plastic work term in the energy balance leading to equation (1) and arrived at a modified Griffith type relationship for the conditions for crack propagation given by

$$\sigma_T \sqrt{c} = \left[\frac{2E(\gamma + \gamma_p)}{\pi} \right]^{\frac{1}{2}} \quad (4)$$

where γ_p is an energy associated with plastic work.

Coble and Parikh²⁸ give a more general discussion of the temperature dependence of the strength of brittle ceramic

materials and they comment that for most pure materials the surface energy decreases with increasing temperature. The fracture strength of sapphire whiskers is also found to decrease with increasing temperature.²⁹ These results are interpreted in terms of fracture without dislocation effects in the low temperature range, fracture accompanied by dislocation nucleation in an intermediate temperature range, and failure associated with dislocation nucleation and motion in the highest temperature range. The brittle fracture strength of fine grained polycrystalline tungsten has also been reported to decrease with increasing temperature.^{30,31} In addition, the temperature dependence of the fracture strength of glass is found to decrease with increasing temperature especially in the low temperature range.³² In this case the temperature dependence is attributed to chemical attack on the surface by surface contaminants. The effect of surface conditions on the mechanical properties of Comp B and TNT are unknown but no evidence of surface sensitivity has been noticed incidental to the studies reported on in this paper. However, the surfaces of all samples were prepared in the same manner, i.e. by machining and without further treatment. The surface treatments of the samples used in the investigations of Clark and Schmitt,^{9,10} and Costain and Motto⁸ are unknown.

The bonding in the various materials discussed immediately above are quite different from the bonding in the molecular

crystalline materials reported on in this paper. Hence, care must be taken in comparing the results discussed immediately above with the results for Comp B and TNT. However, it is clear that the temperature dependence of the compressive strengths of Comp B and TNT can be due at least in part to the temperature dependence of the modulus and the temperature dependence of the fracture surface energy.

The Griffith criterion for fracture, equation (1) or its equivalent, is for catastrophic (instantaneous) crack propagation to fracture. However, many studies have shown that fracture occurs at lower stresses than the value given by equation (1) when a constant stress is maintained for a time t_c .^{33,34,35} The time t_c is generally interpreted as the time required for slow crack growth to obtain a value of crack half length, c_c , which will satisfy an equation like equation (1) for the constant applied stress and thus result in catastrophic crack propagation and failure. The time, t_c , is also temperature dependent and this is generally attributed to thermally activated processes.^{33,34,35} For example, Zhurkov³⁵ has reported an empirical relationship of the form

$$t_c = \tau_0 e^{\left(\frac{U_0 - \gamma \sigma_a}{RT} \right)} \quad (5)$$

where σ_a is the constant applied tensile stress, T is the

temperature in degrees Kelvin, R is the ideal gas constant and τ_0 , U_0 and γ are empirical constants. Equation (5) has been found to describe the dependence of t_c on σ_a and T for about 50 different materials including metals, alloys, non-metallic crystals and polymers³⁵. Zhurkov has further found that the values of τ_0 determined experimentally correspond to the reciprocal of the lattice vibrational frequencies, i.e. values of τ_0 in the vicinity of 10^{-13} s. In addition, he reports that U_0 is in agreement with the heats of sublimation of many metals and in agreement with the energies for thermal decomposition for a number of polymers. Therefore, a simple interpretation is given to equation (5). U_0 is interpreted as the potential energy barrier for "bond" breaking in a solid with no applied stress, and $\gamma\sigma_a$ is taken as the reduction of this potential energy due to the presence of the applied tensile stress. Thus, $U = U_0 - \gamma\sigma_a$ is the effective potential barrier for bond breaking. To relate equation (5) to fracture by crack growth, the rate of crack growth was studied as a function of applied tensile stress in thin polymer strips and found to increase exponentially with stress at a constant temperature. It is straightforward to show that the time to failure as determined in this way is exponentially dependent on applied stress in the same manner as given by equation (5) at

constant temperature. The interpretation given to the parameters of equation (5) seems questionable because t_c should then be the time to break a single bond at the crack tip and not the time to fracture. In addition, $\gamma\sigma_a$ should be a measure of the barrier energy reduction at the crack tip due to the stress at the crack tip and U_0 should be the energy barrier at the crack tip without applied stress and not the heat of sublimation for metals or the heat of thermal decomposition for polymers. However, the empirical nature of equation (5) seems to be firmly established by the data presented by Zhurkov. Stevens and Dutton³⁶ have suggested that the mechanism controlling the fracture processes in the materials reported on by Zhurkov is that of evaporation and condensation. An equation similar to equation (5) has been derived by Beuche for polymers, but with somewhat different meanings ascribed to the parameters³³. However, in a later paper he arrived at a somewhat different equation relating applied tensile stress to temperature and time to failure.³⁷ Hsieh and Thomson³⁸ have considered crack growth in a two dimensional discrete lattice for constant applied stress and also have found that crack growth is a thermally activated process.

In all of the works discussed above the applied stress has been independent of time. Therefore, a direct relationship between these works and the work reported on in this paper cannot

be made because in our case the stress is an increasing function of time. However, for both the low and high strain rate, the time to fracture is found to be independent of temperature within the scatter of the data. Neglecting for the moment the time dependence of the stress σ , we note from equation (5) that for constant t_c we must have

$$U_0 - \gamma\sigma_a = RT \quad (6)$$

and so σ_a must decrease with increasing temperature.

Qualitatively, the effect of having a stress which increases with time (see Figure 2) will be to require more time and so a larger maximum stress than the values for constant stress for slow crack growth to achieve the critical conditions for fracture. Thus, it seems clear that thermally activated slow crack growth will have the effect of decreasing the fracture strength with increasing temperature for Comp B and TNT. To obtain the functional dependence of the fracture strength on temperature would require additional experimental information and assumptions. Charles has extended his work on static loading time to failure to dynamic loading and arrived at a relationship between fracture strength, temperature and loading rate for the case of stress corrosion of glass.³⁹ The dependence of the fracture strength on rate is discussed in the next subsection and some additional discussion of the temperature dependence is also given there.

In summary, it appears that the temperature dependence of the compressive fracture strength can be attributed in part to the temperature dependence of the modulus and in part to thermally activated slow crack growth during loading before fracture. It is also possible that a temperature dependence of the fracture surface energy may play a role.

Strain rate dependence

A reinspection of Figures 7 and 9 shows that the compressive strengths of Comp B and TNT are not only functions of temperature, but also of strain rate and increase with increasing strain rate. As noted above the number of samples measured at each strain rate and temperature are small but the trend as a function of strain rate is clear. The dependence on strain rate is small since an increase of strain rate from $6.7 \times 10^{-4} \text{ s}^{-1}$ to approximately 1.4 s^{-1} , or about a factor 2.1×10^3 , increases the compressive strength only by a factor of approximately two. From equation (1) which results from the Griffith theory of fracture, we note that this rate dependence may be associated with a rate dependence of the modulus and/or the surface energy. It is assumed here that dynamic effects, i.e., the kinetic energy associated with crack propagation, can be neglected. It is also assumed in this discussion that E and γ are constant for a constant strain rate. While the results of this investigation indicate that E is a constant for constant strain rate, the

dependence of γ on strain rate for Comp B and TNT are unknown (see below). It has been found empirically that an equation of the same form as that of equation (1) (see equation (8)) is valid for dynamic loading conditions. Although the data of Figure 8 indicates that the modulus E does increase somewhat with an increase in strain rate, the dependence is even smaller than the dependence of E on temperature. Using equation (3) the fractional change in the compressive strength was calculated due to the observed change in E with strain rate and found to be much less than the observed fractional change in compressive strength. Thus, it is necessary to consider that the change in the compressive strength with a change in strain rate is at least in part due to a change in the fracture surface energy with strain rate. The fracture surface energy has been measured as a function of crack velocity for polymethylmethacrylate and was found to first increase with crack velocity, pass through a maximum and then decrease with further increases in crack velocity.^{40,41} The maximum is attributed to a change from isothermal to adiabatic conditions at the crack tip.⁴⁰ Although the crack velocities for our experimental conditions are unknown, the crack velocities at the low strain rate may correspond to isothermal conditions and thus be related to an increase in fracture surface energy with increasing strain rate if the results cited immediately above can be taken as typical^{40,41}

However, crack velocities at the high strain rate may very well correspond to adiabatic conditions. Measurements of fracture surface energies as a function of strain rate for Comp B and TNT are necessary to resolve this matter.

It is now desirable to consider the role of slow crack growth on the critical conditions for fracture as given by equation (1) or its equivalent for different strain or stress rates. Slow crack growth has been considered in the discussion of the temperature dependence of the compressive strength. For this purpose it is desirable to use the stress intensity factor, K , which is given by

$$K = \sigma\sqrt{cf} \quad (7)$$

where σ is the applied stress, c is the crack half length and f is a dimensionless parameter depending on crack and sample geometry and loading conditions.⁴² The critical stress intensity factor is the value of $K = K_c$ for the conditions of abrupt fracture, that is

$$K_c = \sigma_c\sqrt{c_c}f \quad (8)$$

where σ_c and c_c are the critical applied stress and critical crack length that give abrupt fracture.⁴² Equation (8) is of the same form as the Griffith condition, equation (1).

Charles³⁹ and Evans and associates^{43,44,45} have considered the dependence of the fracture strength on strain rate for glass.

This dependence is associated with a stress corrosion mechanism for glass but the approach is sufficiently general that it can be applied to other mechanisms than stress corrosion. The basic approach of both Charles and Evans is to start with an empirically determined relationship between the crack velocity, v , and the stress intensity factor, K , i.e. the applied stress and the crack half length (equation 7). Since empirical relationships between crack velocity and K are not available for Comp B and TNT, we proceed by assuming such a relationship, and determining its validity by comparing the predicted and observed dependencies of the fracture strength on stress rate. Thus

$$v = \frac{dc}{dt} = AK^n = A \sigma^n \sqrt{c} f^n \quad (9)$$

where A and n are constants for constant temperature. And if

$\sigma = \dot{\sigma}t$, then

$$\int_{c_0}^{c_c} \frac{dc}{\sqrt{c}^n} = Af^n (\dot{\sigma})^n \int_0^{t_f} t^n dt \quad (10)$$

where c_0 is the original crack half length, c_c and t_f are the crack half length and time at fracture and $\dot{\sigma}$ is the stress rate. By integrating we obtain

$$\frac{2}{n-2} \left[\left(\frac{1}{c_c} \right)^{\frac{n-2}{2}} - \left(\frac{1}{c_0} \right)^{\frac{n-2}{2}} \right] = \frac{Af^n (\dot{\sigma})^n t_f^{n+1}}{n+1} \quad (11)$$

for $n \neq 2$. For $n = 2$ the solution is

$$\ln \frac{c_c}{c_0} = \frac{Af^2 (\dot{\sigma})^2 t_f^3}{3} \quad (12)$$

Then we obtain

$$\sigma_c = \sigma t_f = (\dot{\sigma})^{\frac{1}{n+1}} \left[\frac{2(n+1) \left[\left(\frac{1}{c_0} \right)^{\frac{n-2}{2}} - \left(\frac{1}{c_c} \right)^{\frac{n-2}{2}} \right]}{(n-2) Af^n} \right]^{\frac{1}{n+1}} \quad (13)$$

for $n \neq 2$, and for $n = 2$

$$\sigma_c = \dot{\sigma} t_f = (\dot{\sigma})^{\frac{1}{3}} \left[\frac{3 \ln \left(\frac{c_c}{c_0} \right)}{Af^2} \right]^{\frac{1}{3}} \quad (14)$$

If $c_c \gg c_0$, then for the general case of $n \neq 2$

$$\ln \sigma_c = \left(\frac{1}{n+1} \right) \ln (\dot{\sigma}) + F \quad (15)$$

where F is a constant for constant temperature. For the case of

$n = 2$

$$\ln \sigma_c = \frac{1}{3} \ln (\dot{\sigma}) + H \quad (16)$$

where H depends on c_c in addition to c_0 and temperature. Since only two strain rates and so two stress rates were used in this work we have only two points to fit to equations (15) or (16) at a particular temperature for Comp B or TNT. However, Clark and Schmitt⁹ have reported σ_m vs $\dot{\sigma}$ for several stress rates and their data is plotted in Figure 10 along with the two points for the present work and one point from the work of Costain and Motto⁸ for Comp.B. For the Costain and Motto point and the two points of

this investigation the temperature is 23°C. For the work of Clark and Schmitt the temperature is not given but is most probably about the same. If σ_c is taken as σ_m , then a least squares fit to the data points of Clark and Schmitt gives a value of $n = 1.94$. Thus, these results satisfy equation (15) or equation (16) with H very insensitive to c_c and so stress rate if $n = 2$. The results of Clark and Schmitt justify the assumption of equation (9). In the integration of equation (10) to obtain equations (11) and (12) a threshold stress for the onset of slow crack growth was not considered although such a threshold is considered by Evans⁴³ and there is experimental evidence for such a threshold in cases where slow crack growth is related to stress corrosion.^{43,45,46} The fit of the data of Clark and Schmitt to equations (12) or (13) indicates that if there is a threshold it can be neglected for their conditions of measurement. A threshold stress is not indicated in the data for glass in vacuum given by Wiederhorn et. al.⁴⁷ Stress corrosion is not thought to be active in this case. Equation (9) and the subsequent development leading to equations (14) and (15) for constant n is directly applicable only to Region I as discussed by Evans.⁴³ Region II and so Region III are directly related to the process of stress corrosion and are apparently only observed in cases of stress corrosion.^{43,47} For Comp B and TNT there is no evidence for or against stress

corrosion at this time. Measurements in controlled atmospheres and/or measurements of crack velocity as a function of the stress intensity factor, K , are necessary to resolve this matter.

For the two points of the present work and the single point from the work of Costain and Motto a value of $n = 12.5$ is obtained for Comp B. Charles obtained a value of $n = 16$ for Corning 0080 lime glass in saturated water vapor at room temperature while Evans obtained a value of $n = 16$ for soda lime glass in water and $n = 31$ for alumina in air at 50% relative humidity, both at 25°C. The rather large value of n obtained by both Charles and Evans for glass is thought to be related to the corrosive action of water vapor on the crack growth as effected by stress.^{34,48} The crack growth rate in alumina is also apparently related to the presence of water vapor.⁴³ As pointed out by Charles a smaller value of n means more slow crack growth before reaching the critical conditions for rapid crack propagation and fracture (e.g. the Griffith criteria given by equation (1)) and so a larger value of c_c and a smaller value of σ_c as observed (see Figure 10).

The values of n obtained from the data for Comp B given in Figure 7 at 0°C and 60°C are essentially the same as the value obtained at 23°C and the value at 40°C is slightly higher, i.e. $n = 16$. The larger value of n at 40°C is due to the low value of

the compressive strength at the high rate at this temperature (see Figure 7). The values of n for TNT from the data of Figure 9 are about 11 for 23°C, 40°C, and 60°C but a much higher value is obtained at 0°C. An inspection of Figure 9 will reveal that the compressive strengths given at 0°C and the high rate may be low considering the trend as a function of temperature. The large value of n is due to the low values of σ_m at 0°C at the high rate. In general, the low rate compressive strength data of this investigation are in agreement with the values reported by Costain and Motto⁸ (see Figures 7 and 9). Thus, within the scatter of the data, the values of n are independent of temperature over the limited temperature range of this work for both Comp B and TNT. However, it must be noted that only two stress rates were used in this work, and so, even with the additional data of Costain and Motto, the results are not sufficient to firmly establish the kinetic relationship of equation (9) and the subsequent development. Additional measurements as a function of stress rate are needed.

The low rate compressive strengths found in the work of this paper were obtained by the use of closed loop constant strain rate conditions. Thus, the stress rate was constant over the linear portion of the stress vs. strain curve and so almost to failure (see Figure 3). The high rate work was also done in closed loop but the movable crosshead was driven at the maximum

possible velocity. The strain rate and so the stress rate were constant after the initial acceleration for most of the stress vs. strain curve (see Figures 2 and 4). The apparatus used by Costain and Motto should give a constant strain rate, but for the apparatus used by Clark and Schmitt neither the strain rate nor the stress rate are controlled. The apparatus used by these investigators was also used by the present authors to study the mechanical properties of propellants and the apparatus is described briefly in reference 49. An inspection of Figure 3 of reference 49 will reveal that the slopes of the load and deflection vs. time curves are approximately constant after the initial acceleration for the high rate conditions. Thus, the strain and stress rates were most probably roughly constant for the high rate work of Clark and Schmitt. However, it is not clear how the procedure and/or the apparatus was modified by Clark and Schmitt to vary the stress rate to obtain the data as a function of rate.⁹ Thus, no information is available on the profiles of stress (and strain) vs. time curves for the lower stress rates of Figure 10 (lower three points). Possible differences between constant stress rate and constant strain rate are discussed by Evans.⁴³ It seems as if either a different mechanism accounts for the stress rate dependence of σ_r for the samples of Comp B used by Clark and Schmitt ($n \approx 2$) and the mechanism or mechanisms operative in the samples used in this

study and in the work of Costain and Motto ($n = 12.5$), or the samples used by Clark and Schmitt for the lower three stress rate measurements contained significantly larger cracks (larger c_0) than the samples used for the higher rate measurements. While the reasons for the different values of n and so slow crack growth for the data of Clark and Schmitt and the results of the present investigation and that of Costain and Motto are not understood at this time, they could be related to the kinetics of crack initiation.⁴³ For example, if crack initiation must take place before slow crack growth in the samples used in this work and in those used by Costain and Motto but not in the samples used by Clark and Schmitt, then the fracture stress for a given set of conditions of stress rate and temperature will be lower for these latter type of samples as observed. Clearly, additional experimental work is required to resolve this matter.

Before leaving this area of discussion it is appropriate to note that Charles found that there is a thermally activated process associated with slow crack growth, i.e. equation (9) may be rewritten as

$$v = \frac{dc}{dt} = A'e^{-E/RT} \sigma^n \sqrt{c}^n f^n \quad (17)$$

where

$$A = A'e^{-E/RT} \quad (18)$$

The same relationship of crack velocity to temperature has been used for other materials.^{50,51} E is the activation energy and A'

is a constant. Thus, equations (13) and (14) are modified respectively to

$$\sigma_c = (\dot{\sigma})^{\frac{1}{n+1}} \left[\frac{2(n+1) \left[\left(\frac{1}{c_0} \right)^{\frac{n-2}{2}} - \left(\frac{1}{c_c} \right)^{\frac{n-2}{2}} \right]}{(n-2) A' f^n} \right]^{\frac{1}{n+1}} e^{E/RT(n+1)} \quad (19)$$

for $n \neq 2$ and

$$\sigma_c = (\dot{\sigma})^{\frac{1}{3}} \left[\frac{3 \ln \left(\frac{c_c}{c_0} \right)}{A' f^n} \right]^{\frac{1}{3}} e^{E/3RT} \quad (20)$$

for $n = 2$. Equations (19) and (20) indicate a decrease in σ_c with increasing temperature at constant stress rate and an increase in σ_c with increasing stress rate at constant temperature as observed (see Figure 7 and 9). Equation (19) can be fitted approximately to the data for Comp B of Figure 7 for the low and high rates to give a value of $E \approx 30$ kcal/M. This equation can also be fitted to the low and high rate data for TNT of Figure 9 if the data points at 0°C and high rate are omitted to give a value of $E \approx 36$ kcal/M. These values of E are of limited significance because of the limited numbers of measurements and the limited number of temperatures (and stress rates) available to be used in the curve fitting process. However, they are close to the activation energies reported for thermal decomposition of Comp B and TNT, i.e., 39 kcal/M and 27 kcal/M, respectively^{52,53} and so suggest a relationship between crack growth and bond breaking

which is also implicit in the work of Zhurkov.³⁵ This investigator has discussed his experimental results in terms of stress assisted thermally activated bond breaking as noted above. Wiederhorn et.al.⁴⁷ have analyzed their results of slow subcritical crack growth as a function of stress (stress intensity factor K) and temperature for glass in vacuum in terms of stress assisted thermally activated bond breaking and have arrived at a theoretical relationship between these quantities as

$$v = v_0 e^{\frac{(-E + bK)}{RT}} \quad (21)$$

where

$$b = \frac{2}{3} \frac{\Delta V}{\sqrt{\pi} \rho} \quad (22)$$

for the conditions of applied tensile stress and a through elliptical crack. ΔV is the activation volume and ρ is the radius of curvature at the crack tip. Wiederhorn et. al. have fit their data to equation (21) and have obtained values for the activation energies and the activation volumes. A question to be considered is the applicability of equations (9) and (17) vs. equation (21). For equation (21) the crack velocity is exponentially dependent on the stress intensity factor, K , while equations (9) and (17) gives a power law dependence. Evans⁴³ has pointed out that both a power law and an exponential law will fit his data at constant temperature and the power law was chosen because the integration, e.g. equation (10), can in this case be carried analytically. A power law assumption, equation (9), was chosen here for the same

reason. If the exponential form is chosen the integration must be done numerically. However, the exponential form is based on theory, equation (21), whereas the power law is not. If equations (17) and (21) are assumed to be equivalent expressions for the crack velocity, then A' and/or n of equation (17) must be dependent on temperature. However, for the limited available data for Comp B and TNT the exponent n has been found to be independent of temperature and the curve fitting to obtain the activation energies was carried out by assuming that A' is independent of temperature. Additional experiment work is necessary to firmly establish the applicability of equations (9) and (17) to Comp B and TNT and/or to distinguish between equations (17) and (21). Theoretical work is also desirable to establish the bases for equation (17) if in fact this equation is preferred over equation (21).

As pointed out in the Results Section measurements were made at -20° and -40° C but the results were erratic and not reproducible. It is now believed these poor results may have been due to the method of temperature conditioning. Samples were placed in the insulated chamber and solid carbon dioxide was blown in to reach the desired temperature below room temperature for conditioning. In this process the samples were undoubtedly thermally shocked, and this could cause cracking since TNT and Comp B are known to be sensitive to thermal shock.⁵⁴ It seems

very desirable to repeat these measurements using a method of temperature conditioning which does not allow thermal shocking. This will give a wider range of temperatures for determining the applicability of the above equations and, in particular, for determining activation energies and whether they are related to the bond breaking processes active in thermal decomposition. It will also give data over the remaining part of the temperature range of military interest. The apparently low values of compressive strength obtained for TNT at 0°C and high strain rate (Figure 9) are most probably also due to the effect of thermal shocking.

Before leaving the discussion of rate sensitivity the recent work of Sinha is considered.⁵⁵ This investigator developed a constitutive equation for creep at constant load and then, with a few assumptions, applied it to constant strain rate conditions and found agreement between the predictions and the experimental results for columnar grained polycrystalline ice. (Cast TNT has a tendency to be columnar grained.) The stress vs. strain curves as a function of strain rate show the same dependence of the compressive strength, σ_c , and the apparent modulus, E, on strain rate as observed in this work for Comp B and TNT. The total creep strain is taken as made up of three components: i) an elastic term which decreases immediately upon removal of the load; ii) a delayed elastic term which decreases with time after

removal of the load; and iii) a viscous (plastic) term which represents a permanent deformation (strain). The delayed elastic term is attributed to grain boundary sliding which does not lead to cracking and permanent strain and is grain size dependent while the viscous term is due to dislocation motion. This latter term increases with crack generation which occurs when grain boundary sliding displacement reaches a critical value. All cracks are taken to have a constant length which is equal to the grain size. A model for the crack is used in which the crack is represented as an array of dislocations.⁵⁶ The model thus considers crack generation and not crack growth. The resultant stress vs. strain relationship is non-linear and computations were made to obtain stress vs. strain curves as a function of strain rate for a fixed grain boundary size and values of other parameters determined by creep studies. The calculated compressive strengths, σ_m , can be described by a power law relationship with (strain) rate as found for Comp B (see Figure 10), and the strains ϵ_m , are found to be relatively insensitive to strain rate. The results for ice cannot be quantitatively compared to those for Comp B and TNT because parameters obtained from creep studies are needed to make the calculations and creep studies have not been made for these materials. The delayed elastic strain has apparently been observed by Clark and Schmitt¹⁰ for Comp B but there are no measurements or observations of

plastic (permanent) uniaxial deformation that the authors are aware of. In addition, the model does not contain a criterion for fracture and no mention is made of fracture of ice except at the highest strain rate considered which is lower than the lowest strain rate used in the work reported here for Comp B and TNT. Thus, to apply the approach developed by Sinha it would be necessary to add a criterion for fracture, carry out creep studies to obtain the appropriate parameters and, in particular, to determine if there is significant plastic deformation. The average grain size must also be measured.

In summary, the observed rate dependence of the compressive strength may be in part due to (1) rate dependencies of the modulus and the fracture surface energy, (2) thermally activated slow crack growth before fracture and/or (3) crack generation as proposed by Sinha. Additional studies are necessary to further understand these phenomena.

Dependence on Composition

The above discussion has not taken into consideration the effects of composition and microstructure on the compressive strength except for the discussion of the work of Sinha.⁵⁵ The larger compressive strength of Comp B relative to the value of TNT can be attributed at least in part to the effect of second phase particles in Comp B, i.e., RDX particles on the crack path⁵⁰ and the resultant energy loss during crack propagation. TNT

grain size may also play a role. The dependence of the mechanical properties of these materials on composition will be considered in a separate publication.⁵⁷

CONCLUSIONS

The brittle fracture of molecular polycrystalline TNT and the composite Comp B are adequately explained by the Griffith conditions for crack propagation. In particular, the Griffith approach predicts the observed ratios of compressive to tensile strengths, and the general orientation of the fracture surfaces are as predicted. The temperature dependence of the compressive strength can be explained on the bases of the temperature dependence of the modulus, and thermally activated slow crack growth to the critical value necessary for rapid crack growth to fracture, with possibly a contribution by the temperature dependence of the fracture surface energy. The dependence of compressive strength on strain rate is attributed in part to the strain rate dependence of the modulus, in part to the rate of slow crack growth to fracture and/or to the rate of crack generation, with again a possible contribution by the rate dependence of the fracture surface energy. Although experimental results are reported only for TNT and Comp B, these conclusions should apply to the Octols and most if not all other TNT base composites. Additional work is required in almost all areas to more firmly establish the conclusions arrived at in this work.

In particular, more extensive tensile properties are desirable. Measurements at lower temperatures are also desirable to better establish thermally activated crack growth and the associated activation energies and to completely cover the temperature range of military interest. Larger numbers of measurements for each set of conditions are also very desirable. Direct measurements of (slow) crack velocity as a function of stress intensity factor and temperature would definitely aid in the interpretation of the brittle fracture of these types of materials.

ACKNOWLEDGEMENTS

The authors are indebted to D. Georgevich and M. Mezger for assistance with data taking and to M. Mezger, and Y. Lanzerotti for helpful discussions. The authors also wish to thank C. Ribaldo for material characterization, G. Ziegler for casting TNT and Comp B, J. Jenkins for the machining of samples and F. Glanzel for radiographic work.

REFERENCES

1. Pinto, J., Wiegand, D. A., and Nicolaides, S., to be published.
2. Mezger, M. unpublished results.
3. Pinto, J., Nicolaides, S., and Wiegand, D. A., Technical Report ARAED-TR-85004, (1985).
4. Mezger, M., and Wiegand, D. A., unpublished results.
5. Lanzerotti, M. Y. D., and Sharma, J., Appl. Phys. Lett.,

39, 5 (1981).

6. Georgevich, D., private communication.
7. Papoulis, A., "Probability, Random Variables, and Stochastic Processes," Mc-Graw-Hill, NY, (1984), Second Edition, p. 150.
8. Costain T., and Motto, R., Technical Report 4587, Picatinny Arsenal (1973).
9. Clark N., and Schmitt, F., Engineering Sciences Division Information Report No. 558, Picatinny Arsenal (1972).
10. Clark N., and Schmitt, F., unpublished report.
11. U.S. Naval Ordnance Laboratory NAVORD Report 4537. (as quoted by Clark and Schmitt⁹).
12. Dobratz B. M., and Crawford, P. C., LLNL Explosive Handbook; Properties of Chemical Explosives and Explosive Simulants, UCRL-52997, pp 7-8 (1985).
13. See, for example, U.S. Naval Ordnance Laboratory, NAVORD Report 4380 (1956).
14. Griffith, A. A., Phil. Trans. Roy. Soc. (London) Ser. A 221 163 (1921).
15. Griffith, A. A. "Proceedings of the International Congress on Applied Mechanics, Delft," p 55 (1924).
16. Inglis, C. E., Trans. Inst. Naval Architects (London) 60, 219 (1913).
17. Werker, R. E., "Annotated Tables of Elasticity and

- Strength," Petroleum Branch, AIME, N.Y. (1956).
18. Costain, T., private communication.
 19. Obert, L., "Brittle Fracture of Rock" in "Fracture" Vol. VII, ed. Liebowitz, H., Academic Press, New York (1972) pp 130-137.
 20. McClintock, F. A., and Walsh, S. B., In "Proceedings of the 4th U.S. National Congress on Applied Mechanics." Vol. 2. (1962) p 1015.
 21. Coble, R. L., and Parikh, N. M., "Fracture in Polycrystalline Ceramics" in "Fracture", Vol. VII, p 254, ed. Liebowitz H., Academic Press, New York (1972).
 22. See reference 19, pp 143-148.
 23. Sack, R. A., Proc. Phys. Soc. (London) 58, 729 (1946).
 24. See reference 20, pp 261-281.
 25. Congleton, J., and Petch, N. J., Intern. J. Fracture Mechanics, 1, 14 (1965).
 26. See reference 20, p 281.
 27. See for example Orowan, E., "Proceedings of the International Conference in Physics", Vol. 2, p 281, Physics Society (London).
 28. Reference 21, pp 296-307.
 29. Brenner, S. S., J. Appl. Phys. 33, 33 (1962).
 30. Wronski, A. and Fourdeux, A. J., J. Less Common Metals 6, 413 (1964).

31. Valintine, A. P., and Hull, D., *J. Less Common Metals*, 17, 353 (1969).
32. Phillips, C. J., "Fracture of Glass" in "Fracture" Vol. VII, p 24, ed. Liebowitz, H., Academic Press, New York (1972).
33. Bueche, F., *J. Appl. Phys.* 28, 784, (1957).
34. Charles, R. J., *J. Appl. Phys.* 29, 1549 and 1554, (1958).
35. Zhurkov, S. N., *Inter. J. Fracture*, 1, 311 (1965).
36. Stevens, R. N., and Dutton, R., *Mater. Sci. Engr.*, 8, 220 (1971).
37. Bueche, F., *J. Appl. Phys.*, 29, 1231, (1958).
38. Hsieh, C., and Thomson, R., *J. Appl. Phys.* 44, 2061, (1973).
39. Charles, R. J., *J. Appl. Phys.* 29, 1657 (1958).
40. Vincent, P. I., and Gotham, K. V., *Nature*, 210, 1254 (1966).
41. See also Berry, J. P., "Fracture in Polymeric Glasses" in "Fracture" vol. VII, p 65. Liebowitz, H., Academic Press, New York (1972).
42. Ewalds, N. L., and Wanhill, R. S. H., "Fracture Mechanics" Edward Arnold LTT., Baltimore (1984).
43. Evans, A. G., *Inter. J. Fracture*, 10, 251 (1974).
44. Wiederhorn, S. M., Evans, A. G., Fuller, E. R. and Johnson, H., *J. Am. Ceramic Soc.*, 57, 319 (1974).
45. See also Wachtman, J. B. Jr., *J. Am. Ceramics Soc.* 57, 509

- (1974).
46. Wiederhorn, S. M., and Bolz, L. M., J. Am. Ceramic Soc. 53, 543 (1970).
47. Wiederhorn, S. M., Johnson, H., Diness, A. M. and Heuer, A. H., J. Am. Ceramic Soc. 57, 336 (1974).
48. See also Wiederhorn, S. M., J. Am. Ceramic Soc. 50, 407 (1967).
49. Nicoloides, S., Wiegand, D. A., and Pinto, J., Technical Report ARLCD-TR-82010 (1982).
50. Chen, E. P., and Hasselman, D. P. H., J. Am. Ceramic Soc. 59, 525 (1976).
51. Hasselman, D. P. H., and Chen, E. P., J. Am. Ceramic Soc. 60, 76 (1977).
52. Harris, J., Thermochemica Acta, 14, 183 (1976).
53. Harris, J., private communication.
54. Joyce, M., private communication.
55. Sinha, N. K., J. Mater Sci., 23, 4415 (1988).
56. Nicolson, P. S., High Temp. Sci., 13, 279 (1980).
57. Pinto, J., Wiegand, D. A., and Nicoloides, S., to be published.

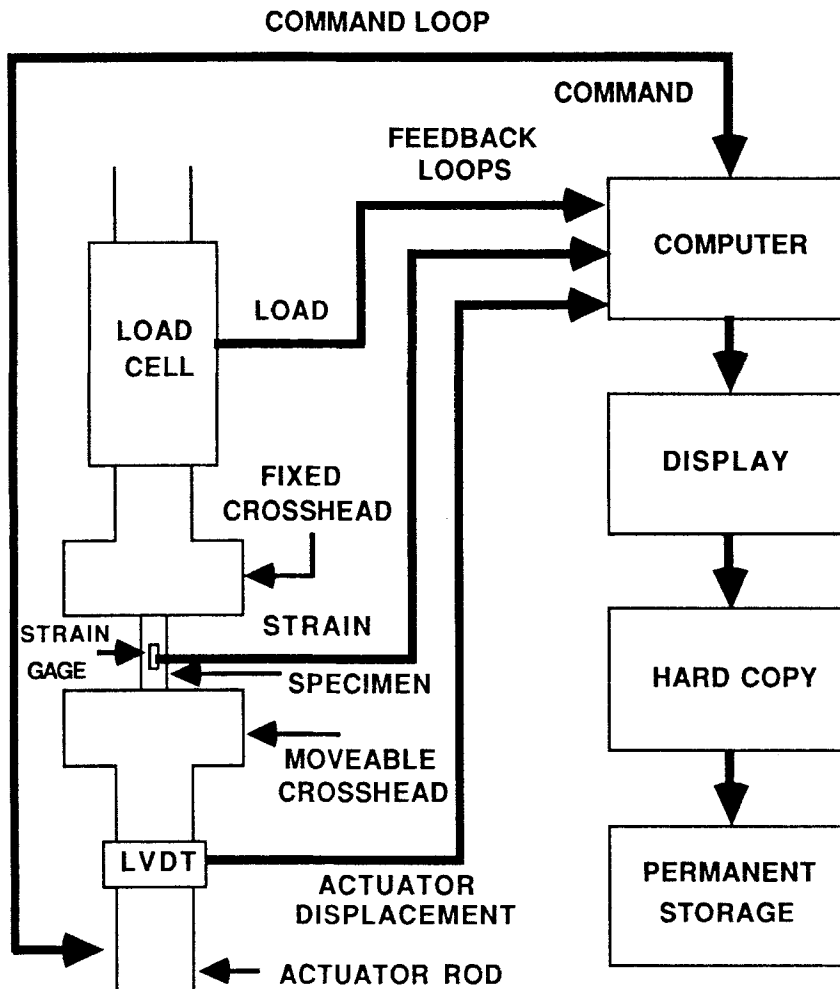


FIGURE 1

Block Diagram of the Servo-Hydraulic Loading System and the Electronics.

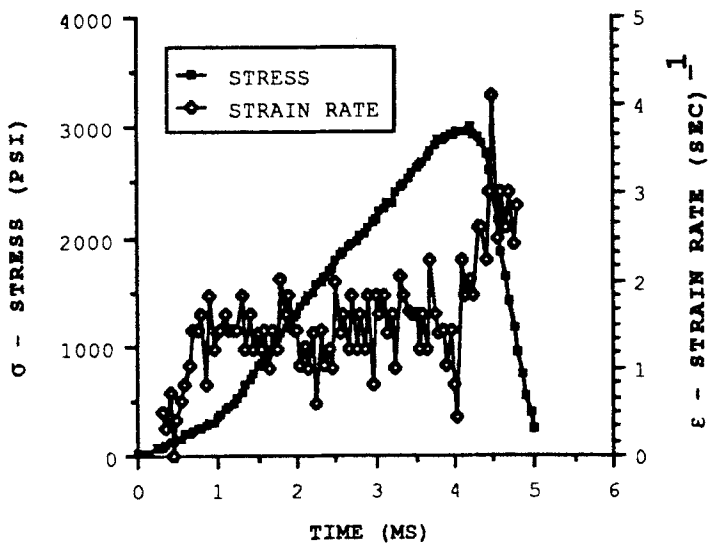


FIGURE 2

Typical stress and strain rate vs. time for the high strain rate for Comp B at 23°C.

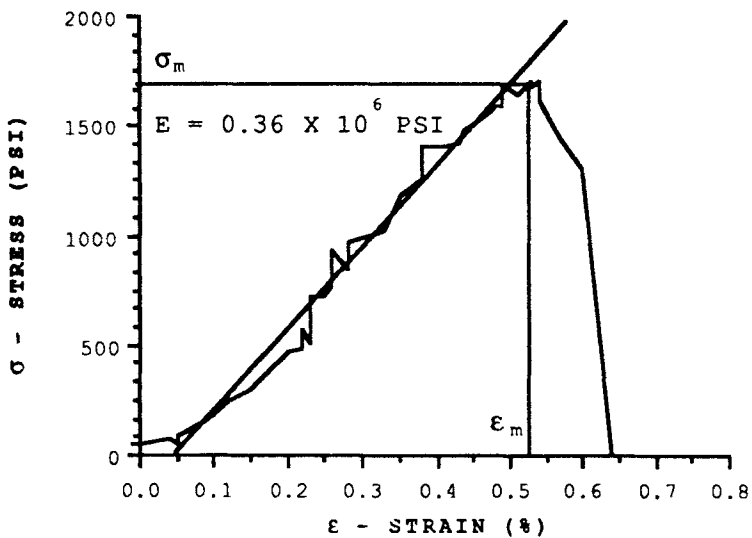


FIGURE 3

A stress vs. strain curve for Comp B at 23°C and the low strain rate, showing the values of the compressive strength, σ_m , Young's Modulus, E, and the strain, ϵ_m .

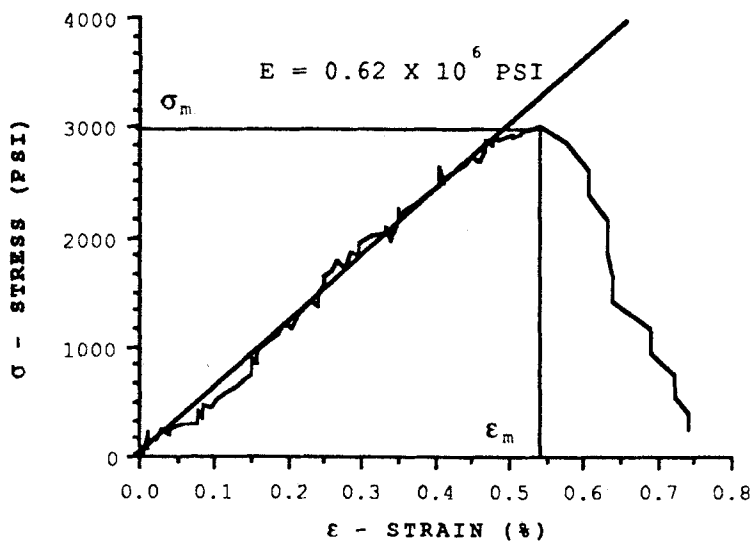


FIGURE 4

A typical stress vs. strain curve for Comp B at 23°C and the high strain rate, showing the values of the compressive strength, σ_m , Young's Modulus, E , and the strain, ϵ_m .



FIGURE 5

Typical fragments of Comp B after fracture.

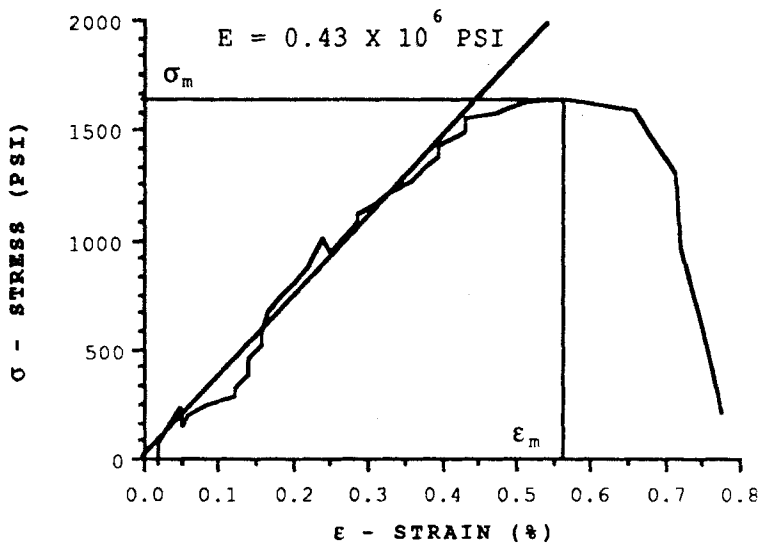


FIGURE 6

A typical stress vs. strain curve for TNT at 23°C and the high strain rate, showing the values of the compressive strength, σ_m , Young's Modulus, E, and the strain, ϵ_m .

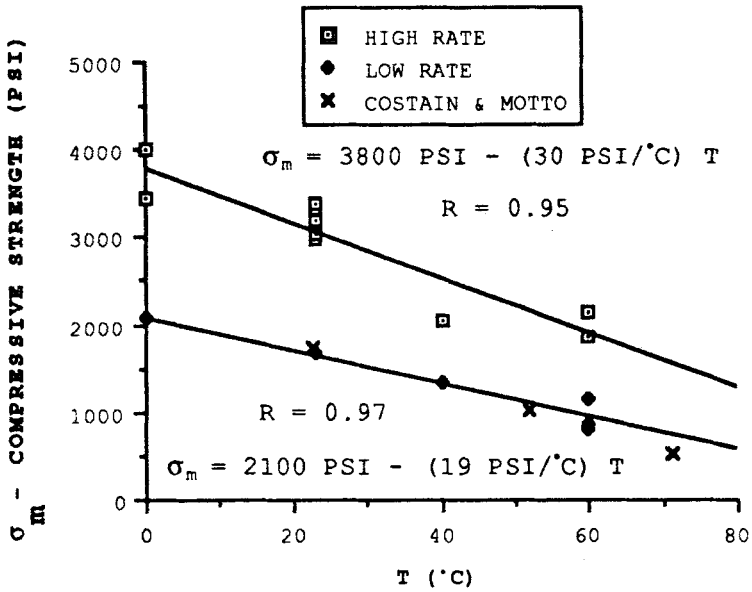


FIGURE 7

Compressive strength, σ -, vs. temperature for Comp B for the low and high strain rates. The lines are least squares fits of straight lines to the data points. R is the correlation coefficient.⁷ Also shown are points from the work of Costain and Motto.⁸

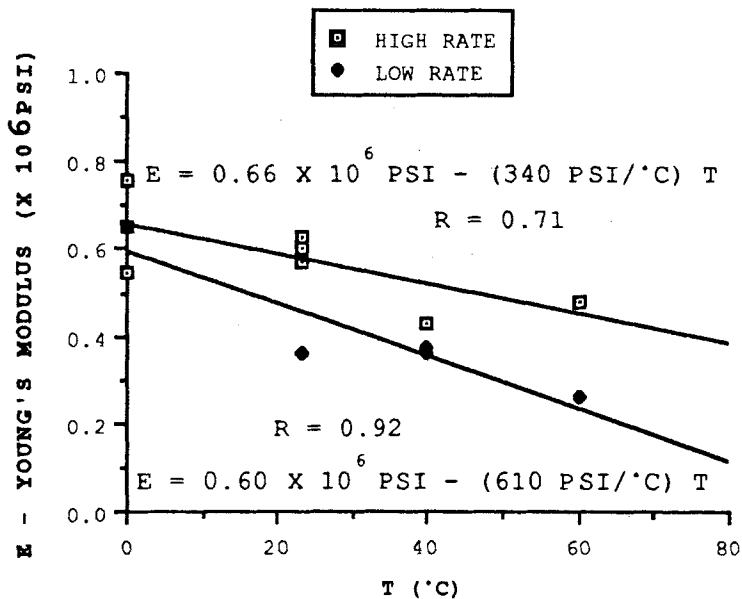


FIGURE 8

Young's Modulus, E , vs. temperature for Comp B at the low and high strain rates. The lines are least squares fits of straight lines to the data points. R is the correlation coefficient.⁷

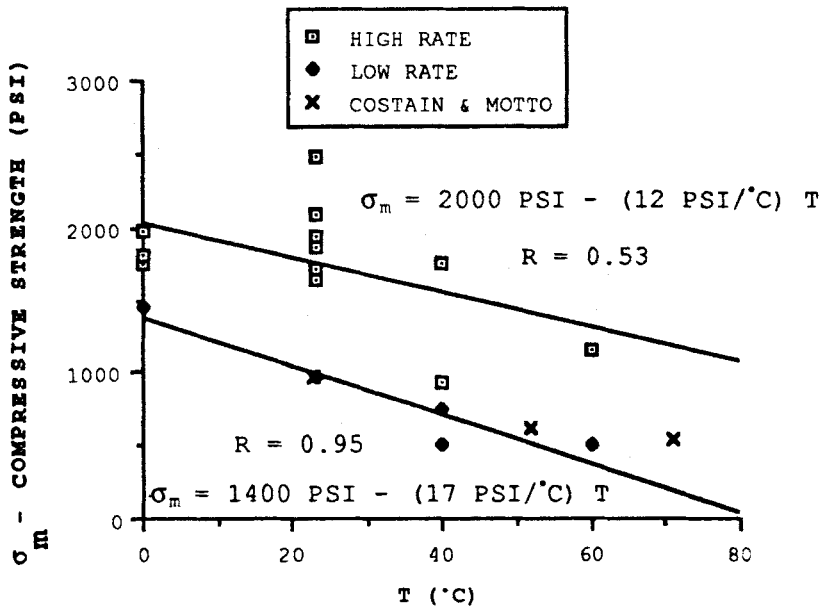


FIGURE 9

Compressive strength, σ_m , vs. temperature for TNT for the low and high strain rates. The lines are least squares fits of straight lines to the data points. R is the correlation coefficient.⁷ Also shown are points from the work of Costain and Motto.⁸

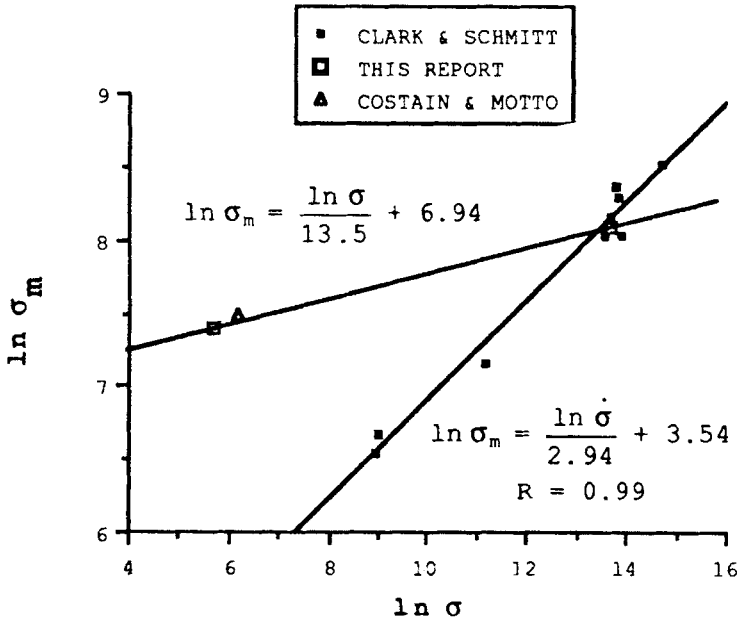


FIGURE 10

The natural logarithm of the compressive strength, σ_m vs. the natural logarithm of the compressive stress rate, $\dot{\sigma}$, for Comp B. Data are presented from the work of Clark and Schmitt, from the work of Costain and Motto⁹ and from the present investigation. The line through the data of Clark and Schmitt is a least squares fit of a straight line to the data points. A straight line is also drawn through the two data points of the present investigation. R is the correlation coefficient.⁷